Available online at www.sciencedirect.com

ScienceDirect

Journal of Magnesium and Alloys 6 (2018) 384–389

www.elsevier.com/locate/jma

Full Length Article

Effect of Si addition on microstructure and wear properties of Mg-Sn as-cast alloys

Erdem Karakulak[a,1,*], Yusuf Burak Küçüker[b]

[a] *Kocaeli University, Faculty of Engineering, Department of Metallurgical and Materials Engineering, 41380 Kocaeli, Turkey*
[b] *AKKAR Silah Sanayi, Orhanli Mah., 34956 Istanbul, Turkey*

Received 28 June 2018; received in revised form 15 August 2018; accepted 29 August 2018
Available online 17 September 2018

Abstract

Effect of Si addition on microstructure, hardness and wear resistance of as cast Mg-5Sn and Mg-10Sn alloys were investigated. For this purpose alloys with wt.-% 0, 0.5, 1, 1.5 Si were cast using an induction furnace. Addition of Si to both alloys caused an increasement in the amount of intermetallic phases at the grain boundaries. Also refined grain structure was reported with increasing Si content in the cast alloys. Both increased amount of intermetallics and decreased grain size caused an increase in the hardness of the alloys. Wear resistance of the binary alloys first increased with Si addition and then decreased. Increased amounts of Si in the alloys caused crack formation during wear tests and decreased wear resistance. Sliding speed also has a dramatical effect on the wear resistance of the alloys. Increased sliding speed resulted with higher wear resistance. Worn surfaces of the alloys also investigated under scanning electron microscope to understand the wear mechanisms operated during wear tests.

Keywords: Magnesium; Casting; Microstructure; Hardness; Wear.

1. Introduction

The need for weight reduction in different applications like automotive or aviation causes a search for lighter structural materials. Magnesium and its alloys can fulfill this role because of their low density and high strength to weight ratio [1–4]. Although there are some Mg alloys that can compete with Al alloys and common steels, more development is required in strength and corrosion resistance of magnesium alloys to increase their usage in different applications [5–7]. In the last two decades Mg-Sn based alloys are of special interest. Sn has a high solubility limit in Mg at high temperatures and this solubility limit decreases with decreasing temperature which makes this alloys suitable for precipitation hardening treatment [8,9]. Addition of Sn to Mg causes formation of Mg_2Sn phase, this phase has a melting point of 770 °C and can effect mechanical properties of the alloy at elevated temperature positively [10]. Rare earth (RE) elements also form stable precipitates and also improve high temperature properties [11,12]. However these elements are high in cost which limits applications of RE containing alloys. Sn is reasonably cheap compared with RE elements [13]. Because of this promising situtation a number of studies have been conducted on different Mg-Sn based alloys. Effects of different alloying elements like Ca, Zn, Al, Si, Nd, In, Bi, Y and Mn [14–19] on different properties of binary Mg-Sn alloys have been investigated by different researchers. Although the microstructures, mechanical properties, corrosion properties and heat treatments of Mg-Sn based alloys have been investigated in detail [20–26] there are limited information about wear properties of these alloys. Poddar et al. investigated wear characteristics of some gravity die-cast and rheo-cast Mg-Sn based alloys [27,28]. Whereas Jiang et al. studied

* Corresponding author.
E-mail addresses: erdemkarakulak@kocaeli.edu.tr, Erdem.Karakulak@brunel.ac.uk (E. Karakulak).
[1] Present address: BCAST Brunel University London, Uxbridge, Middlesex UB8 3PH, UK

https://doi.org/10.1016/j.jma.2018.08.004

wear behaviour of extruded Mg-Sn-Yb alloys [29]. Improving wear resistance of magnesium alloys can increase their usage in different applications especially in automotive industry. This study aims to understand effects of Si addition on microstructure, hardness and wear properties of two binary Mg-Sn alloys with different Si contents.

2. Experimental

In this study Mg-Sn alloys with two different Sn content and four different Si content was cast to understand the effect of Si on microstructure and wear resistance of the materials. An induction furnace with a graphite crucible was used for the casting operations. Commercially pure Mg (99.8 wt.-%), Sn (99.7 wt.-%) and Si (99.6 wt.-%) were used in the experiments. All melting processes were conducted under Ar atmosphere. First Mg-5Sn and Mg-10Sn alloys were produced. Then parts were cut from these cast materials and remelted. Different amounts of silicon were (wt.-% 0, 0.5, 1, 1.5) added to the melts and then the specimens were cast into metal mold with dimensions of $50 \times 30 \times 150$ mm, preheated to 150 °C. Samples were cut 50 mm from the bottom of the castings and used in experiments. Chemical compositions of all investigated samples were measured using an optical emission spectrometer. Cast samples were ground with silicon carbide papers and then polished with diamond paste. Polished samples were etched using an etchant consisting of 5 ml acetic acid, 6 g picric acid, 10 ml water and 100 ml ethanol. Microstructural investigations were concluded using an Olympus BX41M-LED ligth microscope and a Jeol JSM 6060 scanning electron microscope (SEM) with an energy dispersive X-ray spectrometer (EDS). Grain size measurements were done using line interception method on the images taken with light microscope. All reported grain size values are average of the measurements taken from ten images per alloy. Phases in the cast materials were identified using a Rigaku SA-HF3 X-Ray difractometer with Cu K-α radiation at 40 kV and 40 mA, using a step scan (0.02°/step) of 2θ from 10° to 90° with a scanning speed of 1°/min. Hardness tests were realized according to ASTM E384-11 using a Future-Tech Vickers hardness tester under 1 kg load [30]. All reported hardness values are an average of ten measurements. Wear tests were performed on polished samples at room temperature using a Nanovea MT/60/NI ball-on-disc type tribometer according to ASTM G99-05 [31]. Normal load was selected as 20 N for all wear tests, AISI 52,100 steel balls (5 mm in diameter and approximately 800 HV hardness) were used as counterfaces. The sliding distance were kept constant for all tests as 1000 m whereas two different sliding speeds were selected for wear tests, namely 0.4 and 0.8 m/s. Samples were cleaned with alcohol and dried with hot air before and after tests. The weight loss of the samples were measured using an AND GR200 microbalance. Obtained wear loss values were used to calculate wear rate of the alloys, calculation of the wear rate is explained elsewhere [32]. Worn surfaces of the materials were also investigated using SEM to understand the active wear mechanisms.

Table 1.
Chemical compositions of the cast alloys (wt.-%).

Element	Sn	Si	Al	Fe	Mg
Mg-5Sn	5,09	0,04	0,11	0,02	Balance
Mg-5Sn-0,5Si	4,95	0,48	0,09	0,03	Balance
Mg-5Sn-1Si	4,82	1,03	0,08	0,03	Balance
Mg-5Sn-1,5Si	5,01	1,42	0,10	0,02	Balance
Mg-10Sn	9,92	0,03	0,11	0,03	Balance
Mg-10Sn-0,5Si	10,03	0,52	0,09	0,02	Balance
Mg-10Sn-1Si	10,08	1,05	0,10	0,02	Balance
Mg-10Sn-1,5Si	9,91	1,52	0,10	0,03	Balance

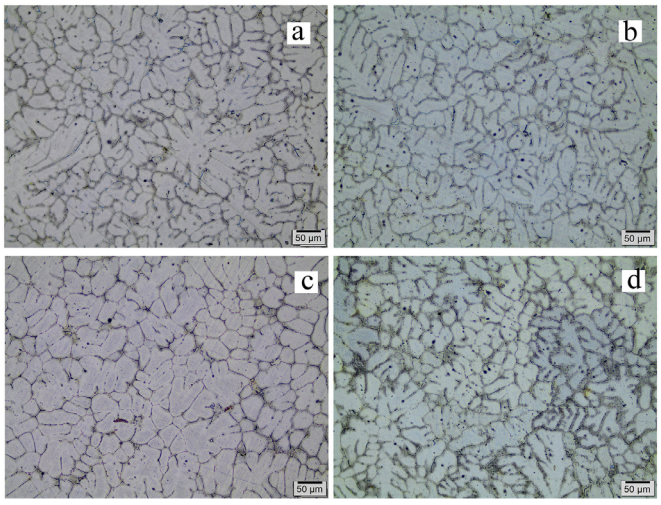

Fig. 1. Microstructures of Mg-5Sn alloys with (a) 0, (b) 0.5, (c) 1.0 and (d) 1.5 Si addition.

3. Results

3.1. Microstructural investigations

Results of the chemical analyses of the samples are given in Table 1. Microstructural investigations of the alloys showed that all alloys have dendrite like grain structure. The microstructure of the alloys consist of α-Mg dentrites and intermetallic phases at grain boundaries of these dentrites. Microstructures of all investigated alloys are given in Figs. 1 and 2.

It is also evident that addition of silicon to both Mg-5Sn and Mg-10Sn binary alloys causes an increase in the amount of the intermetallics at the grain boundaries. Also increament of tin content from wt.-% 5 to 10 causes formation of higher amount of phases in the grain boundaries of dendritic α-Mg grains. Amount of the secondary phases in the alloys were quantified using an image analysis software. For each alloy ten images were analysed and the average values were calculated. Amounts of the secondary phases according to the alloy composition is depicted in Fig. 3.

SEM imaging and EDS analysis of the phases in the microstructures were performed on selected as-cast samples. As can be seen on Fig. 4 increasing tin content in the alloy increases volume fraction of intermetallic phases. All the grain boundaries of Mg-10Sn-1.5Si alloy is surrounded by these

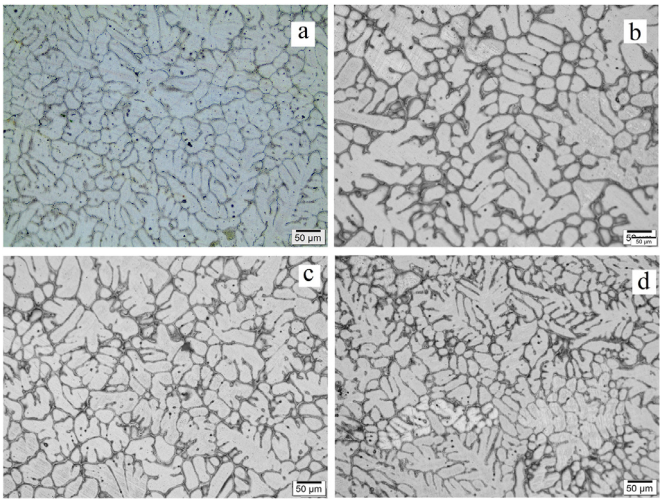

Fig. 2. Microstructures of Mg-10Sn alloys with (a) 0, (b) 0.5, (c) 1.0 and (d) 1.5 Si addition.

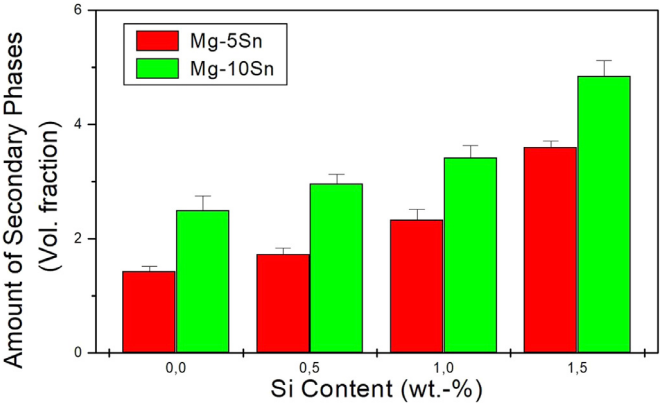

Fig. 3. Amount of the secondary phases with increasing alloying additions.

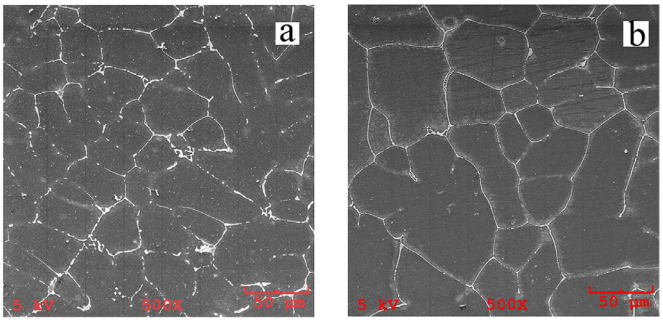

Fig. 4. SEM images of (a) Mg-5Sn-1.5Si and (b) Mg-10Sn-1.5Si alloys.

intermetallics (Fig. 4.b). Whereas some grain boundaries are free of intermetallics on the Mg-5Sn-1.5Si alloy (Fig. 4.a). Segregation of alloying elements in the regions close to the grain boundaries is also visible in the microstrustures of the alloys. Increased amount of alloying elements causes more segregation during solidification.

According to the binary Mg-Sn phase diagram addition of Sn to Mg causes precipitation of Mg_2Sn intermetallic phase. On the other hand according to the previous studies addition

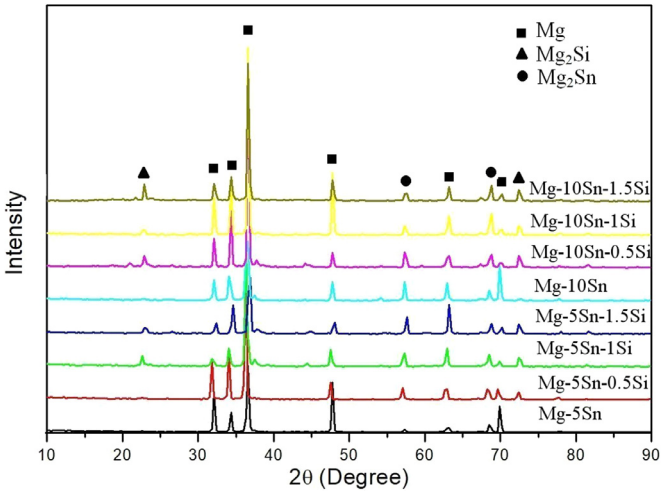

Fig. 5. XRD patterns of the cast alloys.

of Si to Mg-Sn alloys causes precipitation of Mg_2Si phase and in Mg-Sn-Si alloy system there is no ternary intermetallic compounds were reported [33]. X-ray diffraction analysis were conducted to identify these phases and the results of the analysis can be seen on Fig. 5. XRD patterns of binary Mg-Sn alloys show the existence of Mg and Mg_2Sn phases. On the other hand addition of Si to Mg-Sn binary alloys results with formaton of Mg_2Si intermetallic phase. It is known that there is an extensive solid solubility between Mg_2Sn and Mg_2Si phases [34]. Because of that the intermetallics in the grain boundaries can contain different amount of silicon. Some of the EDS analysis results of different phases on the microstructure and the points where these analysis were taken are shown in Fig 6.

3.2. Grain size measurements

Effect of tin and silicon content on the grain size of the alloys can be seen on Fig 7. The grain size of the alloys decreases with increasing Si content. Also Mg-10Sn alloy has smaller avarage grain size compared to Mg-5Sn alloys for all silicon contents. The reason of the decrease in the grain size with increasing alloying element content can be expalined by interdependence theory. In the light of recent research grain size of a cast material is related to the potency of nucleant particles and solute segregation in the liquid solid interface [35,36]. Potency of nucleant particles are related to the properties of these particles (size, surface roughness, etc). On the other hand solute segregation in the solidification front increases undercooling and can help more particles to act as nucleants. Also segregation of solute atoms to the solidification front has a restricting effect on the grain growth. This effect is different for different solute atoms and defined as growth restriction factor (Q). Growth restriction factor can be calculated for different solute atoms using $Q = m_l C_0(k-1)$ formula, where m_l is the slope of the liquidus line, C_0 is the composition of the alloy and k is the partition coefficient. In magnesium Si has a $m_l(k-1)$ value equal to 9.25 which is the

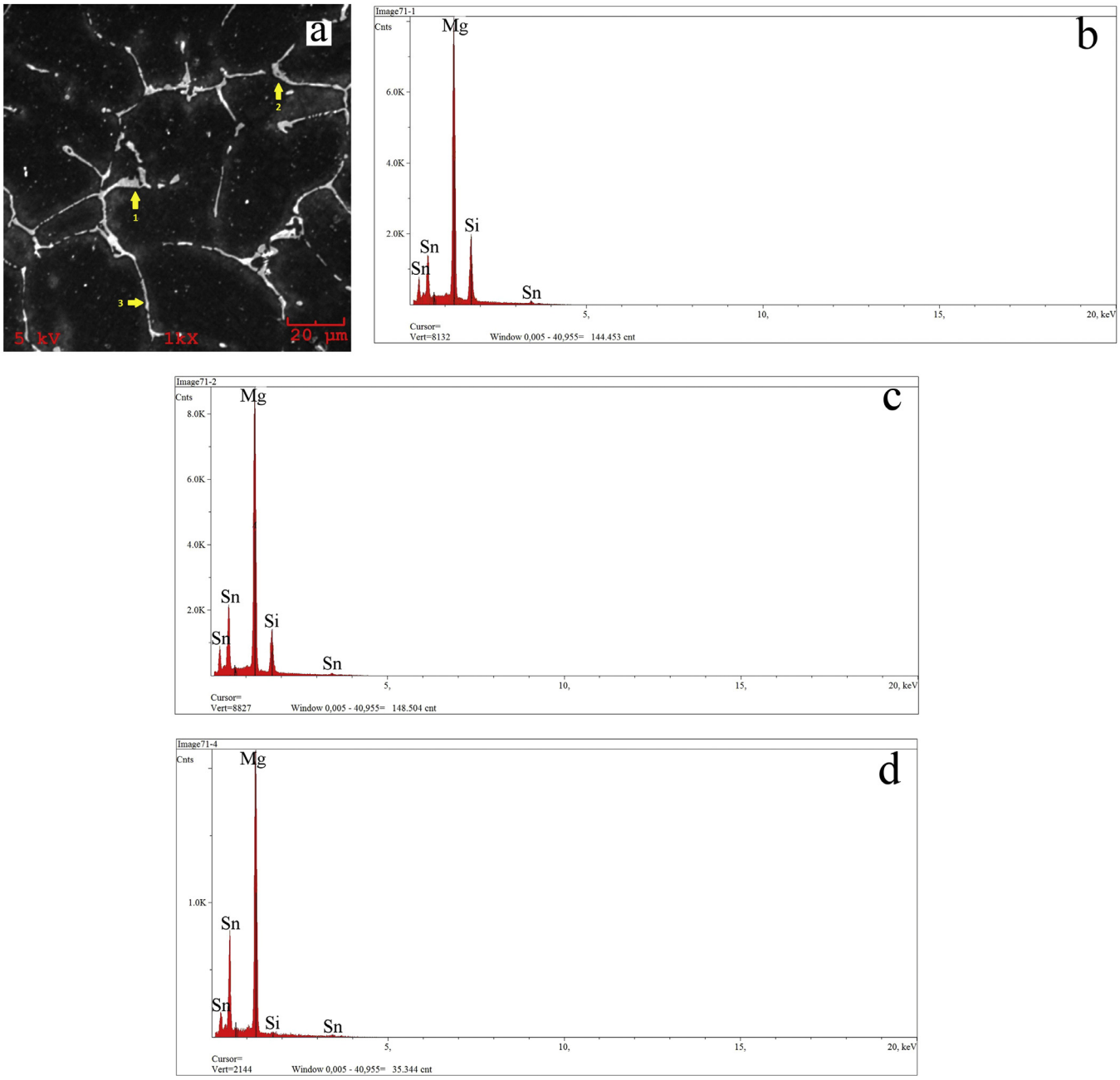

Fig. 6. (a) SEM image of Mg-10Sn-1.5Si alloy and EDX analysis of the phases on the microstructure.

highest fourth value after Fe, Zr and Ca [37]. This means addition of even small amounts of Si to Mg alloys can result with higher grain restriction effect and decreased grain size. Although Sn has a lower Q value which is equal to 1.47 increasing Sn content from 5% to 10% also has a refining effect on the grain size of the material [37].

3.3. Hardness measurements

Fig. 8 shows change of the hardness of Mg-5Sn and Mg-10Sn alloys with silicon addition. Hardness of the alloys increases almost linearly with increasing silicon content. The increase in the hardness of the alloys is result of two different mechanisms. Addition of Si causes formation of Mg_2Si intermetallic phases with relatively high hardness compared to Mg matrix. Increasing amount of Si in the alloy increasses volume fraction of Mg_2Si intermetallics and increases hardness. On the other hand addition of Si to the binary alloys causes a decrease in the grain size of the alloys as can be seen on Fig. 7. When grain size of a metallic material is decreased hardness of the material increases according to well known Hall-Petch equation.

3.4. Wear tests

Wear rate values of different alloys can be seen on Fig. 9. For both Mg-5Sn and Mg-10Sn alloys addition of silicon first increased wear resistance but when Si content is

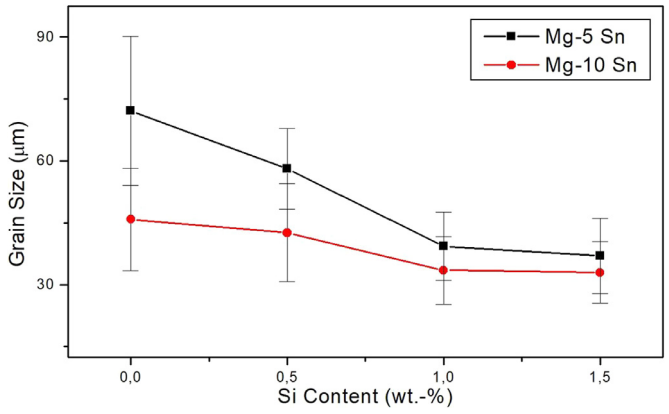

Fig. 7. Change of grain size of Mg-5Sn and Mg-10Sn alloys with Si addition.

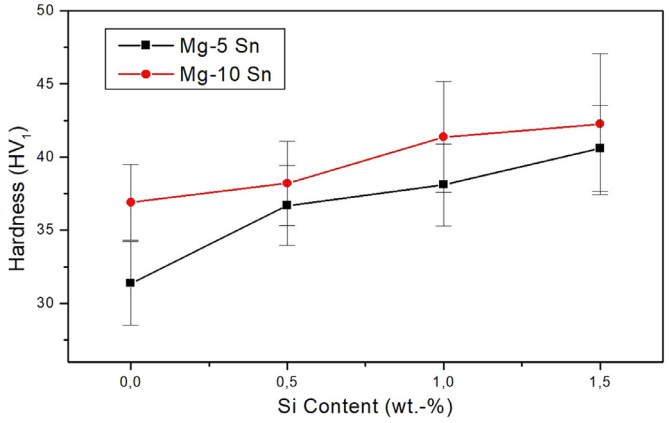

Fig. 8. Effect of Si addition on the hardness of the alloys.

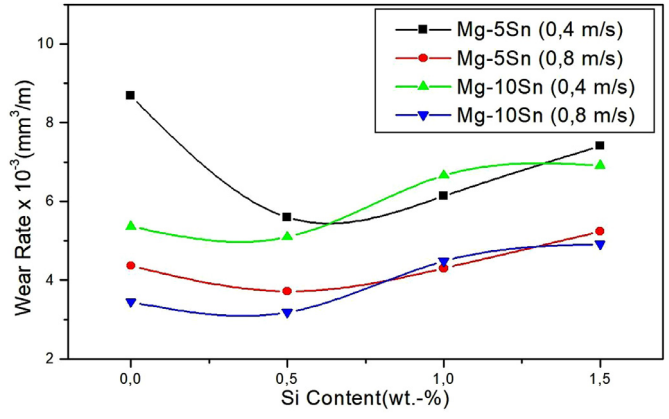

Fig. 9. Wear rate values of Mg-5Sn-xSi and Mg-10Sn-xSi alloys tested with different sliding speeds.

1% or higher wear resistance of the alloy is effected negatively. It is obvious from both graphs that sliding speed has a dramatical effect on the wear resistance of the Mg-Sn-Si alloys. As can be seen on the graphs for all alloys increased sliding speed during wear tests results with decreased wear rate. When Mg-5Sn and Mg-10Sn alloys with same Si content is compared, for all silicon values Mg-10Sn alloys has lower wear rate.

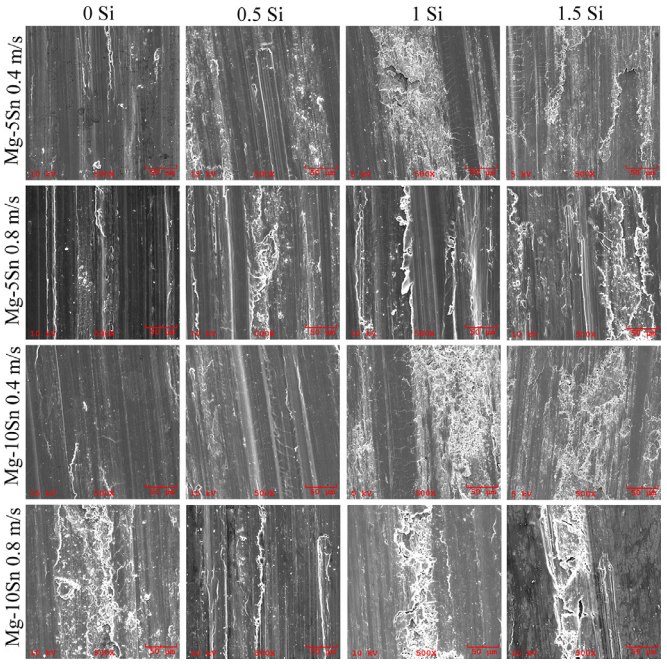

Fig. 10. SEM images of worn surfaces of specimens after wear tests.

3.5. Worn surface investigations

Worn surfaces of the samples after wear tests were investigated under SEM to understand the operating wear mechanisms. Representative images of the worn surfaces can be seen on Fig. 10. Grooves with different depths were reported on the worn surface of binary Mg-Sn alloys for all two Sn contents and for all two sliding speeds. These grooves are result of the abrassive wear caused by the movement of relatively hard counterface on the surface of softer specimens. Addition of 0.5% Si causes a decrease in the number of grooves and existing grooves are shallower. Further increasing silicon content in the alloys causes formation of cracks on the worn surface. Coalescence of these cracks results with removal of materials from the specimen during wear tests. As a result wear rate of the material increases. Increased Si content in the alloys causes an increase in the volume fraction of the Mg_2Si intermetallic phases. These intermetallic phases are hard and fragile and usually cause crack formation and propagation during wear tests.

It is also reported that worn surfaces of the alloys tested with higher sliding speed shows higher oxidation tendency. Increased sliding speed causes more friction during wear tests which results with increased heat formation. When the temperature in the interface increases higher levels of oxidation occurs. Although oxidation is a wear mechanism, in some cases formation of oxides on the worn surface may help to decrease wear rate of the alloy. During wear tests plastic deformation of the matrix can cause distribution of produced oxide particles in the material which results with a composite-like structure. Introduction of hard oxide particles in soft Mg matrix increases wear resistance of the material. Fig. 11 shows oxide particles with different sizes that mixed with the matrix

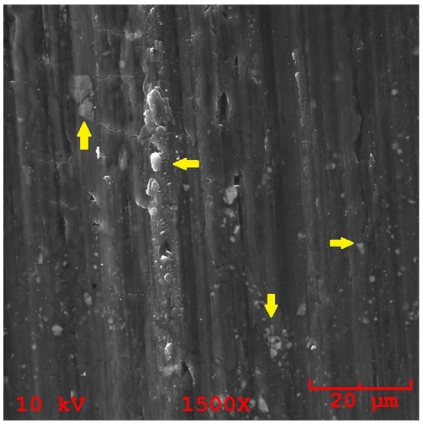

Fig. 11. SEM image of worn surface of Mg-10Sn-1Si alloy tested with a sliding speed of 0.8 m/s.

during wear test. The layer formed with distribution of oxides during wear test is called as Mechanical Mixing Layer (MML) [38,39]. Formation of MML during the wear tests with 0.8 m/s sliding speed can explain the lower wear rate values of all alloys tested at higher sliding speeds.

4. Conclusions

In this study Mg-5Sn and Mg-10Sn alloys with different Si contents were cast. Microstructural investigations, grain size measurements, hardness and wear tests were conducted on the cast samples. Also worn surfaces of the specimens were investigated. Following conclusions can be drawn from the results of the experimental work.

- Increasing Sn content in the alloys and addition of Si causes an increasement in the amount of intermetallic phases in the grain boundaries of the alloys.
- With increasing amounts of alloying elements (both Sn or Si) in the alloy grain size decreases.
- Addition of Si to binary alloys increases hardness. Also alloys with high Sn content have higher hardness compared to the ones with lower Sn content.
- For all Sn contents maximum wear resistance of the alloy is obtained with 0.5% silicon addition.
- Sliding speed during wear tests has an enormous effect on the wear rate of the materials. Increased sliding speeds results with higher wear resistance.
- Abrassive wear was dominant for the binary alloys whereas crack fromation and removal of material was reported for the alloys with high Si content. Increased sliding speed caused higher oxidation levels on the worn surfaces of the specimens.

References

[1] L. Guo, F. Zhang, L. Song, R.C. Zeng, S.Q. Li, E.H. Han, Surf. Coat. Technol. 328(2017) 121–133.
[2] S. Pawar, T.J.A. Slater, T.L. Burnett, T. Zhou, G.M. Scamans, Z. Fan, G.E. Thompson, P.J. Withers, Acta Mater. 133 (2017) 90–99.
[3] P. Cheng, Y. Zhao, R. Lu, H. Hou, Z. Bu, F. Yan, Mater. Sci. Eng., A. 708 (2017) 482–491.
[4] D. Zhang, D. Zhang, F. Bu, X. Li, B. Li, T. Yan, K. Guan, Q.Q. Yang, X. Liu, J. Meng, Excellent ductility and strong work hardening effect of as-cast Mg-Zn-Zr-Yb alloy at room temperature, J. Alloys Compd. 728 (2017) 404–412.
[5] S. You, Y. Huang, K.U. Kainer, N. Hort, J. Magnesium Alloys. 5 (2017) 239–253.
[6] G.P. Abatti, A.T.N. Pires, A. Spinelli, N. Scharnagl, T.F. Conceicao, J. Alloys Compd. 738 (2018) 224–232.
[7] H. Bolin, Y. Yingxia, X. Songsong, L. Zongmin, Rare Met. Mater. Eng., 46(2017) 17–22.
[8] T. Hu, W. Xiao, F. Wang, Y. Li, S. Lyu, R. Zheng, C. Ma, J. Alloys Compd. 735 (2018) 1494–1504.
[9] C.Q. Liu, H.W. Chen, H. Liu, X.J. Zhao, J.F. Nie, Acta Mater. 144 (2018) 590–600.
[10] P. Poddar, K.L. Sahoo, Mater. Sci. Eng., A. 556 (2012) 891–905.
[11] W. Han, G. Yang, L. Xiao, J. Li, W. Jie, Mater. Sci. Eng., A. 684 (2017) 90–100.
[12] S.M. Zhu, T.B. Abbott, M.A. Gibson, J.F. Nie, M.A. Easton, Mater. Sci. Eng., A. 682 (2017) 535–541.
[13] C. Zhao, X. Chen, F. Pan, S. Gao, D. Zhao, X. Liu, Mater. Sci. Eng., A. 713 (2018) 244–252.
[14] J. Kubasek, D. Vojtech, J. Lipov, T. Ruml, Mater. Sci. Eng., C. 33 (2013) 2421–2432.
[15] T. Abu Leil, N. Hort, W. Dietzel, C. Blawert, Y. Huang, K.U. Kainer, K.P. Rao, Trans. Nonferrous Met. Soc. China. 19 (2009) 40–44.
[16] M. Keyvani, R. Mahmudi, G. Nayyeri, Mater. Sci. Eng., A. 527 (2010) 7714–7718.
[17] H. Pan, G. Qin, M. Xu, H. Fu, Y. Ren, F. Pa, Z. Gao, C. Zhao, Q. Yang, J. She, B. Song, Mater. Des. 83 (2015) 736–744.
[18] P. Poddar, K.L. Shoo, S. Mukherjee, A.K. Ray, Mater. Sci. Eng., A. 545 (2012) 103–110.
[19] Q. Wang, Y. Chen, S. Xiao, X. Zhangi, Y. Tang, S. Wei, Y. Zhao, J. Rare Earths. 28 (2010) 790–793.
[20] Y. Chen, Y. Wang, J. Gao, J. Alloys Compd. 740 (2018) 727–734.
[21] Y. Wang, J. Peng, L. Zhong, J. Alloys Compd. 744 (2018) 234–242.
[22] F.R. Elsayed, T.T. Sasaki, C.L. Mendis, T. Ohkubo, K. Hono, Mater. Sci. Eng., A. 566 (2013) 22–29.
[23] P. Poddar, A. Kamaraj, A.P. Murugesan, S. Bagui, K.L. Sahoo, J. Magnesium Alloys. 5 (2017) 348–354.
[24] B.Q. Shi, R.S. Chen, W. Ke, J. Alloys Compd. 509 (2011) 3357–3362.
[25] H. Fu, J. Guo, W. Wu, B. Liu, Q. Peng, Mater. Lett. 157 (2015) 172–175.
[26] K. Suresh, K.P. Rao, Y.V.R.K. Prasadi N. Hort, K.U. Kainer, Trans. Nonferrous Met. Soc. China. 23 (2013) 3604–3610.
[27] P. Poddar, A. Das, K.L. Sahoo, Metall. Mater. Trans. A. 45A (2014) 2270–2283.
[28] P. Poddar, A. Das, K.L. Sahoo, Mater. Des. 54 (2014) 820–830.
[29] J. Jiang, G. Bi, L. Zhao, R. Li, J. Lian, Z. Jiang, J. Rare Earths. 33 (2015) 77–85.
[30] ASTM E384 - 11, Standard Test Method for Knoop and Vickers Hardness of Materials, Am. Soc. Test. Mater. 2011.
[31] ASTM G99 - 05, Standard Test Method for Wear Testing with a Pin-on-Disk Apparatus, Am. Soc. Test. Mater. 2005.
[32] R. Yamanoglu, E. Karakulak, M. Zeren, F.G. Koc, Int. J. Cast met. Res. 26 (2013) 289–295.
[33] I.H. Jung, D.H. Kang, W.J. Park, N.J. Kim, S.H. Ahn, Claphad: Comput. Coupling Phase Diagrams Thermochem 31 (2007) 192–200.
[34] A. Kozlov, J. Grobner, R. Schmid-Fetzer, J. Alloys Compd. 509 (2011) 3326–3337.
[35] M.A. Easton, M. Qian, A Prasad, D. StJohn, Curr. Opin. Solid State Mater. Sci. 20 (2016) 13–24.
[36] D.H. StJohn, M. Qian, M.A. Easton, P. Cao, Acta Mater. 59 (2011) 4907–4921.
[37] D.H. StJohn, M. Qian, M.A. Easton, P. Cao, Z. Hildebrand, Metall. Mater. Trans. A. 36A (2005) 1669–1679.
[38] S.C. Sharma, B. Anand, M. Krishna, Wear. 241 (2000) 33–40.
[39] K.S. Prakas, P. Balasundar, S. Nagaraja, P.M. Gopal, V. Kavimani, J. Magnesium Alloys. 4 (2016) 197–206.